

Supplemental information

Pepper variome reveals the history and key loci associated with fruit domestication and diversification

Yacong Cao, Kang Zhang, Hailong Yu, Shumin Chen, Donghui Xu, Hong Zhao, Zhenghai Zhang, Yinqing Yang, Xiaozhen Gu, Xinyan Liu, Haiping Wang, Yaxin Jing, Yajie Mei, Xiang Wang, Véronique Lefebvre, Weili Zhang, Yuan Jin, Dongliang An, Risheng Wang, Paul Bosland, Xixiang Li, Ilan Paran, Baoxi Zhang, Giovanni Giuliano, Lihao Wang, and Feng Cheng

1 **Supplementary Information for**

2

3 **Pepper variome reveals the history and key loci associated with fruit domestication and**
4 **diversification**

5

6 Yacong Cao^{1†}, Kang Zhang^{1†}, Hailong Yu^{1†}, Shumin Chen^{1†}, Donghui Xu^{1†}, Hong Zhao¹, Zhenghai
7 Zhang¹, Yinqing Yang¹, Xiaozhen Gu¹, Xinyan Liu¹, Haiping Wang¹, Yaxin Jing¹, Yajie Mei¹, Xiang
8 Wang¹, Véronique Lefebvre², Weili Zhang¹, Yuan Jin¹, Dongliang An¹, Risheng Wang³, Paul Bosland⁴,
9 Xixiang Li¹, Ilan Paran⁵, Baoxi Zhang¹, Giovanni Giuliano^{6*}, Lihao Wang^{1*}, Feng Cheng^{1*}

10 *Feng Cheng, Lihao Wang, Giovanni Giuliano

11 **Email:** chengfeng@caas.cn, wanglihao@caas.cn, giovanni.giuliano@enea.it

12

13

14 **This file includes:**

15 Complete version of **Materials and Methods**

16 **Supplementary Tables S3, S4, S6, and S7**

17 **Supplementary Figures S1 to S13**

18 **SI References**

19

20 **Another file as a spreadsheet includes:**

21 **Supplementary Tables S1, S2, and S5**

22

23

24 **Materials and Methods**

25

26 ***Pepper sample collection***

27 A total of 347 pepper accessions were used in this study, including the core collection of the China
28 Gene Bank (Gu et al., 2019; Wang et al., 2018), core breeding inbred lines of Institute of Vegetables
29 and Flowers, and international typical local varieties and wild species. In total, 12 species were
30 collected, including 309 *C. annuum* (cultivated species), two *C. annuum* var. *glabriusculum* (wild
31 species), 10 *C. frutescens* (cultivated species), 10 *C. chinense* (cultivated species), five *C. baccatum*
32 (cultivated species), one *C. baccatum* var. *baccatum* (wild species), two *C. pubescens* (cultivated
33 species), one *C. cardenasii* (wild species), two *C. chacoense* (wild species), one *C. eximium* (wild
34 species), one *C. flexuosum* (wild species), one *C. galapagoense* (wild species), one *C. minutiflorum*
35 (wild species), and one *C. rhomboideum* (wild species). Samples originated from the Americas, Europe,
36 Asia, and Africa and were obtained from several genebanks.

37

38 ***Agricultural characteristics investigation***

39 The experimental materials were planted five times, including a greenhouse in Langfang during spring
40 2016; in a greenhouse in Beijing, in a plastic greenhouse in Dehong, and in the open field of Urumqi
41 during spring 2017; and in the open field of Urumqi during spring 2018. Three replicates were planted
42 in each experiment. In the Langfang and Beijing experiments, two to three plants were planted, and two
43 fruits were measured in each replicate; and in Dehong and Urumqi experiments, 10 plants were planted,
44 and 10 fruits were measured in each replicate.

45 The mature fruit traits measured were as follows: (1) fruit length: the distance from the pedicel
46 attachment to the fruit apex; (2) fruit diameter: the maximum width; (3) fruit shape index - the ratio of
47 fruit length to fruit diameter; (4) fruit orientation - if the fruit points upward, it is recorded as erect,
48 otherwise it is recorded as pendent; (5) the content of capsaicin and dihydrocapsaicin of dried fruits
49 without seeds and pedicels, as measured by ultra-performance liquid chromatography (UPLC).

50 For the measurements of capsaicin and dihydrocapsaicin, mature fruits without seeds and pedicels
51 were dried at 55 to 60°C for about two days, ground and processed according to an improved agricultural
52 industry standard (NY/T 1381-2007, Determination of Capsaicin by high-performance liquid
53 chromatography [HPLC]). For each determination, 0.2 g (accurate to 0.0001 g) of sample powder was
54 extracted with 25 mL of methanol-tetrahydrofuran (1:1) (HPLC-grade; Sigma, USA) solution, shaken,
55 extracted in an ultrasonic extractor for 30 min in a 60°C water bath, and then filtered. The filter residue
56 and filter paper were re-extracted with 25 mL methanol-tetrahydrofuran solution in an ultrasonic
57 extractor for 10 min, filtered, and then the above operation was repeated. The three collected filtrates
58 were combined, concentrated on a rotary evaporator (70–75°C water bath) to about 30 mL, and then
59 transferred to a 50 mL volumetric flask, where methanol was added to produce the final volume. After
60 being filtered through a 0.22- μ m micron organic phase filter membrane, chromatographic analysis was
61 performed. The capsaicin content in the test solution was diluted to 0.13 mg/L–160 mg/L, and the
62 dihydrocapsaicin content was diluted to 0.04 mg/L–160 mg/L. The filtrate was injected into a UPLC
63 system (Waters UPLC, USA) with an ACQUITY UPLC BEH C18 1.7 μ m, 2.1*100 mm column
64 (Waters, USA) and Photo Diode Array Detector. The mixture of methanol and distilled water (70:30)
65 represented the mobile phase. The flow rate was 0.20 mL/min. The injection volume was 2 μ L, and the
66 column temperature was 30°C. The detection wavelength was at 280 nm, and the retention times were
67 3.276 min for capsaicin and 4.395 min for dihydrocapsaicin. Capsaicin and dihydrocapsaicin external
68 standards (Sigma, USA) were prepared as 200 mg/L stocks in absolute methanol. The stock solution
69 was diluted with methanol to a series of standard working solutions of 100 mg/L, 50 mg/L, 20 mg/L,
70 10 mg/L, 1 mg/L, and 0.2 mg/L, and measured under the above liquid chromatography conditions. With

71 the concentration of capsaicin and dihydrocapsaicin as the ordinate, and the corresponding peak area
72 integral as the abscissa, the standard curves and linear regression equations were calculated. After the
73 prepared test solution was measured, it was calibrated at multiple points and quantified by the peak area
74 integral values. Finally, the capsaicin and dihydrocapsaicin contents were converted into mg per kg dry
75 weight.

76

77 ***DNA extraction, library construction, and sequencing***

78 The DNA library was prepared according to the manufacturer's instructions (NEBNext® UltraTM
79 DNA Library Prep Kit for Illumina®). The adaptor-ligated DNA was cleaned with the MinElute
80 Reaction Cleanup Kit instead of Vortex AMPure XP Beads. After PCR amplification, the PCR products
81 were assessed on 2% agarose electrophoresis. Next, quantitative analysis of the DNA library was
82 conducted with a Qubit 2.0 (Invitrogen, USA) and an Agilent 2100 Bioanalyzer (Agilent, USA). All
83 the libraries with 300 bp insert size were sequenced on the Illumina Solexa platform, and 150 bp paired-
84 end reads were generated.

85

86 ***PacBio HiFi Sequencing***

87 Genomic DNA was extracted from the leaves of Zunla-1 using the Blood & Cell Culture DNA Kit .We
88 used 30µl high quality genomic DNA to construct a SMRT bell target size library using the PacBio
89 SMRT bell template prep kit. The constructed library was sequenced on the PacBio Sequel II platform
90 using the circular consensus sequencing (CCS) mode at Berry Genomics. A total of 32.54 Gb of raw
91 HiFi sequencing reads with the N50 length of 20.25 kb were obtained.

92

93 ***Genome gap closing***

94 The assembly gaps in the Zunla-1 genome was closed using the generated HiFi reads. Specifically, the
95 HiFi data was equally divided into four parts. TGS-GapCloser (Xu et al., 2020) (parameter: "--scaff --
96 minimap_arg '-x asm20' --racon -tgstype pb") was used to fill the gaps with four rounds based on the
97 four parts of data.

98

99 ***Protein-coding gene prediction***

100 Prediction of the protein-coding genes in the gap-closed Zunla-1 genome was performed according to
101 the previously described method (Yang et al., 2022). Briefly, the results from homology-based searches,
102 mRNA-seq assisted prediction, and *ab initio* prediction were integrated using EVIDENCEModeler
103 (version 1.1.1)(Haas et al., 2008). In the homology-based prediction process, protein sequences of
104 eleven species (pepper, Arabidopsis, cacao, coffee, eggplant, grape, petunia, potato, snapdragon,
105 tobacco, and tomato) were collected and were aligned to the updated Zunla-1 genome to identify the
106 homologous genes using Exonerate (version 2.4.7)(Guy St C and Ewan, 2005). The RNA-seq data
107 obtained from previous study (Qin et al., 2014) was used for mRNA-seq assisted prediction. The *ab*
108 *initio* gene prediction was performed using GeneMark (version 4.61_lic) (Lomsadze et al., 2005) and
109 Augustus (version 3.3.3) (Hoff and Stanke, 2018).

110

111 ***Variants calling and annotation***

112 Trimmomatic v0.33 trimmed the Illumina fastq raw reads and removed adapters based on the
113 manufacturer's adapter sequences to obtain clean reads. Clean reads were mapped to the Zunla-1 2.0
114 genome (Qin et al., 2014) using BWA 0.7.17 (Li and Durbin, 2009) with the following parameters:
115 mem -M -A 1 -B 4 -O 6 -E 1. Samtools was used to sort the sam files and convert them into bam files.
116 The function MarkDuplicates integrated in GATK (version 4.1.7) was used to deduplicate the bam files.

117 Then, variants were called out using the HaplotypeCaller function of GATK with default parameters
118 and generated the raw VCF files. Variant loci that were ungenotyped in more than 40% of the 311 *C.*
119 *annuum* accessions, as well as those loci with a heterozygosity ratio of more than 10% and a minor
120 allele frequency < 5% in the *C. annum* population, were further filtered by an in-house Perl script. The
121 genotype information of these remaining reliable variant loci in the 311 accessions of *C. annum* and
122 37 accessions from other *Capsicum* species were then obtained for further data analysis. By doing this,
123 we reduced the bulk and biased variants resulting from the large genetic difference between the genomes
124 of *C. annum* and the other *Capsicum* species. Furthermore, the ANNOVAR (Wang et al., 2010b) was
125 used to annotate variant function. Based on annotated data, SNPs and InDels were classified according
126 to their position in or outside genes as being in: (1) inter-genic regions. (2) CDS (coding sequences)
127 regions, (3) intronic regions, and (4) UTR (untranslated regions) (both 5' and 3'). Variants in CDS were
128 subdivided into two groups: one group causing changes to the coding amino acids, including non-
129 synonymous SNPs and non-threefold frame shift InDels, and another group with synonymous SNPs
130 and InDels without frame-shifts. Intronic variants were divided into two groups: splice site mutations
131 (within 2 bp of the splice site) and others.

132 The CNVs (copy number variations) and PAVs (presence/absence variations) were called out
133 using the CNVnator (Abyzov et al., 2011) and Control-FREEC (Boeva et al., 2012). To reduce the false
134 positives, only the accessions with resequencing depth $\geq 8\times$ (123 in total) were selected for the analysis.
135 There were 23 accessions that eventually failed to meet the criterion ($4 \leq SD \leq 5$) in CNVnator when a
136 wide range of bin sizes were used. These accessions were therefore excluded from further analyses,
137 while for the retained 100 accessions, the bin sizes were set as 800–1200 bp, which were varied in
138 different accessions, to optimize the SD value. For Control-FREEC, the window and the step sizes were
139 set as 1200 bp and 600 bp, respectively. These two tools were run separately, and only the intersections
140 of detected intervals were retained. The results were further refined by merging the variants with
141 reciprocal overlap $\geq 80\%$. Finally, variants with frequency < 3 or > 80 in the 100 accessions were
142 filtered out.

143 144 ***Frequency distribution of variants***

145 To estimate the density of the variants in the pepper genome, the number of various types of SNPs and
146 InDels were counted in a one Mb sliding window across the 12 chromosomes of pepper, and the results
147 were drawn in a genomic circos plot using the Circos tool (Krzywinski et al., 2009).

148 For the frequency of average variants in the gene body and the flanking regions of the gene, firstly
149 the 5 kb regions flanking each gene were determined. When the flanking region overlapped with the
150 gene body or flanking region of another gene, the process was stopped at the middle site in the two
151 neighboring genes. A one kb sliding window with a 100 bp step screened the flanking regions and gene
152 body of all pepper genes, and the number of SNPs and InDels located in the window were calculated.
153 After that, each of these windows were further averaged across all the genes, and the upper and lower
154 quartiles were calculated.

155 156 ***KASP genotype verification***

157 Kompetitive Allele Specific PCR (KASP) verified the SNPs. The SNPs were randomly selected for the
158 KASP assay, and primers were designed using BatchPrimer3 online (You et al., 2008)
159 (<https://probes.pw.usda.gov/batchprimer3/>). The allele-specific forward primers allele 1 and allele 2
160 carried the FAM- and HEX-labeled tails with the targeted SNP at the 3' end. A common reverse primer
161 was designed to amplify the 80–200 bp target region. The test operation mainly followed the #KBS-
162 1016-017 (Laboratory of the Government Chemist, UK) instructions (www.lgcgroup.com/genomics)
163 and was as follows: 1) DNA samples were arrayed into 384-well PCR plate. No-template controls are

164 included on each plate; 2) to prepare the genotyping mix, 2.0 μ L DNA (10–50 ng/ μ L), 2.0 μ L 2 \times KASP
165 Master mix, 0.055 μ L KASP Assay mix were combined. The total reaction volume was 4 μ L; 3) the
166 genotyping mix was dispensed onto the reaction plate, to which 2.0 μ L genotyping mix was added to
167 each DNA sample in the reaction plate using a pipette; 4) the plate was sealed and centrifuged; 5) the
168 thermal cycle was run in the Roche LightCycler 480 System[®]. The cycle included an initial
169 denaturation step of 15 min at 94 $^{\circ}$ C, followed by 10 touchdown cycles of 20 s at 94 $^{\circ}$ C and 60 s at 61 $^{\circ}$ C,
170 then decreasing by -0.6° C per cycle, followed by 26 cycles of 20 s at 94 $^{\circ}$ C and 60 s at 55 $^{\circ}$ C, and nine
171 additional cycles of 20 s at 94 $^{\circ}$ C and 60 s at 57 $^{\circ}$ C. 6) the plate was then read, and the data were analyzed.
172 After completion of the thermal cycle, the reaction plate was read in a FRET-capable platter reader at
173 37 $^{\circ}$ C. The LightCycler 480 Software[®] was used to analyze the data. The result was assessed based on
174 the difference between the cycle threshold (Ct) values of the two alleles. The greater the difference, the
175 greater the possibility of a pure gene (determine its allele according to the type of fluorescent substance
176 connected by the special primers), and the smaller the difference, the more likely it was heterozygous.

177

178 ***Phylogenetic tree construction***

179 In order to select neutral and reliable SNP variants to investigate the phylogenetic relationships of the
180 resequenced pepper accessions, these genic SNPs that were annotated as synonymous variations by
181 ANNOVAR were extracted (Wang *et al.*, 2010b). It was determined that 165,864 such SNPs were in
182 the 347 resequenced pepper accessions. The distance matrixes with the genotype data for all 347 pepper
183 accessions was generated. Within the 311 *C. annuum* accessions the pairwise allele sharing distance
184 (ASD) was calculated for each pair of two accessions, and the data in the distance matrix were used to
185 construct a neighbor-joining (NJ) phylogenetic tree using PHYLIP3.69 (Retief, 2000).

186

187 ***Population structure analysis***

188 The software Admixture (version 1.3.0) (Pritchard *et al.*, 2000) performed genetic structure analyses
189 using 160,000 randomly selected SNPs from the 311 *C. annuum* accessions. Admixture was run with k
190 = 2–15 clusters with the default parameters. Finally, $k = 7$ (seven major genetic components, **Fig. 1d**)
191 that showed the smallest CV error was selected to represent the population genetic features of *C.*
192 *annuum*.

193

194 ***Linkage disequilibrium***

195 Correlation coefficients (r^2) were calculated for each pair of SNP loci with a distance of 1–500 kb
196 between them and averaged per bin of 50 bp distance, producing a histogram of r^2 per such distance
197 bin. From these histograms, the distance at which r^2 decayed to half its maximum value was determined
198 as a linkage disequilibrium (LD) length estimate of a particular sample group.

199

200 ***Determination of ancestral and derived alleles***

201 In order to estimate the frequency of genotype status—ancestral or non-ancestral (derived)—of the SNP
202 variants and compare them in different groups of pepper, the ancestral/derived alleles for each SNP
203 locus were determined. To obtain a reliable genotype status, the genotypes of the two wild *C. annuum*
204 var. *glabriusculum* samples were used as the controls. Only the homozygous SNP locus shared by the
205 two samples were retained. We then recorded the genotype of the two wild samples as the ancestral
206 allele of the SNP locus, while the other allele in the pepper population at this SNP locus was recorded
207 as the derived one. With this rule, the ancestral/derived alleles of 14,194,356 SNPs out of the 18,372,022
208 total SNPs were successfully obtained. The information of derived alleles of these SNPs was used in
209 the data analysis.

210

211 ***Genome diversity and selection sweeps***

212 Two measures were used to estimate the genomic diversity of the *C. annuum* population: π and ROD
213 (reduction of diversity). The π measures the genomic diversity (Tajima, 1983) through computing the
214 average difference per locus on each pair of accessions. While ROD is a measure based on π , which
215 estimates the diversity reduction of a sample group with respect to the control sample group (Xu et al.,
216 2011). In this study, ROD detected the genomic regions under group-specific selection as compared to
217 the parental group.

218 Akey's F_{ST} calculated the pairwise genomic differentiation between two groups of samples (Akey
219 et al., 2002), which evaluates the strength of genomic divergence between two compared groups. Values
220 ranged from 0 (no differentiation) to 1 (complete or fixed differentiation).

221 XP-EHH detected signals of recent positive selection (group-specific selection signatures) (Sabeti
222 et al., 2007) in the blocky fruit group of *C. annuum*, using the combined software of Beagle (version
223 5.1) (Browning et al., 2018) and SelScan (version v1.3.0) (Szpiech and Hernandez, 2014), with default
224 parameters. Large XP-EHH values indicate unusually long haplotypes in the derived group under
225 selection as compared to the control group. Tajima's D was applied to estimate genomic regions under
226 negative selection/purifying selection, and outliers were detected with a threshold of less than -2
227 (Tajima, 1989).

228 To obtain the strongest selection signals from the large genome of pepper (3.6 Gb), which is
229 comparatively larger than most crop genomes sequenced, the calculated values of these population
230 genomic measures were further averaged using a 10 Mb window with a 1 Mb increment sliding across
231 the whole genome of pepper, except for Tajima's D, which was calculated directly in each sliding
232 window. The top 5% of ROD and XP-EHH were determined as outlier signals of genomic regions under
233 selection. If two outlier windows overlapped with each other, then they were merged into one region.

234

235 ***Selection strength on gene units***

236 The gene body combined with its 5 kb upstream and 5 kb downstream regions were defined as a gene
237 unit, and 35,336 such gene units were generated using the Zunla-1 genome (version 2.0) as the reference
238 (Qin et al., 2014). Measures of π and ROD (Xu et al., 2011) were then calculated using SNP variants
239 located at each of these gene units, which were further used to estimate the gene level selection strength
240 in the pepper population. The top 5% of ROD values, together with the top 30% of smaller π values in
241 the control group, were determined as outliers of gene units that were under selection.

242

243 ***Major haplotype sharing analysis***

244 The major haplotypes in the blocky fruit groups were first determined using a 10 Mb window with 1
245 Mb increment sliding across the 12 chromosomes of the pepper reference genome. In total, there were
246 548 such windows. In each window, the major allele frequency of each SNP in the blocky fruit pepper
247 was calculated, and the SNP loci with a value ≥ 0.8 were counted and collected. If more than 80% of the
248 SNPs in the window were counted, then these major alleles comprise the major haplotype of the blocky
249 fruit groups in the analysed window. These major haplotypes were kept and compared to all of these
250 resequenced *C. annuum* accessions. The average score of allele sharing between the major haplotype
251 and each of the 311 accessions in the analyzed window was calculated and considered as a major
252 haplotype sharing score (MHS). The MHS then estimated the relationship on the origin of the blocky
253 fruit pepper-specific haplotype in the pepper population.

254

255 ***K_S analysis***

256 In order to obtain the gene sequences for blocky fruit pepper, the consensus genome of blocky fruit
257 pepper by replacing the Zunla-1 reference genome was generated (Qin *et al.*, 2014) using the major
258 genotype of blocky fruit pepper at each variant locus. Gene sequences of blocky fruit pepper were
259 extracted based on the gene annotation coordinate file. After that, pairwise protein sequences between
260 blocky fruit pepper and Zunla-1 (non-blocky fruit pepper) were aligned by MUSCLE (Edgar, 2004).
261 Protein alignments were translated into coding sequence alignments using an in-house Perl script. The
262 *K_S* values were calculated with the coding sequence alignments using the method of Nei and Gojobori
263 as integrated in the KaKs_calculator (Wang *et al.*, 2010a).

264

265 ***GWAS analysis***

266 GEMMA (Zhou and Stephens, 2012) was applied to perform GWAS. The relatedness (kinship) matrix
267 was first calculated by GEMMA and applied to correct the pepper population stratification in the 311
268 accessions of *C. annuum*. The linear mixed model (LMM) analyzed the correlation of the population,
269 and *P*-values of all SNPs to each trait were generated by GEMMA. The GWAS signals of traits analysed
270 in this study are replicable in the five phenotypic trials, and GWAS results on the averaged values of
271 the five trials were used to make the Manhattan plotting.

272

273 ***Validation of associations in another pepper population***

274 The candidate genes were then further validated in another 241 *C. annuum* accessions. According to
275 the mutation types, different types of primers were developed. For SNPs related to the fruit shape index,
276 primers spanning the SNP were designed (F: GGAGGTCAGACGTGGATCATC, R:
277 TGATGGTTTGTGGTTTGAGCA) and the genotype was determined by the PCR products
278 sequencing using the forward primer as the sequencing primer. For structural variations related to fruit
279 orientation, primers that span the variation segment were designed (F:
280 GTGCTGCAAGAGGAAGAAAAC, R: CAGCCCTCTTTTCCTTGTATG), and the genotype was
281 determined by the PCR-amplified fragment size indicated by polyacrylamide gel and agarose gel
282 electrophoresis, respectively.

283

284 ***RNA-Seq and data analysis***

285 For transcriptome sequencing, 22 accessions of various fruit types and 10 accessions with different
286 pungency levels were selected. The pericarp from accessions with various fruit types at the early stage
287 about 5 to 7 d after pollination, and then about 15 to 20 d after pollination, the placenta of different
288 pungency levels at the middle stage of fruit development were sampled and immediately placed into
289 liquid nitrogen for more than 30 s, then they were stored in an ultra-low temperature refrigerator at -
290 80°C until sequencing. The RNA-Seq data were mapped to the genome of Zunla-1 (version 2.0) (Qin
291 *et al.*, 2014) using the software Hisat2 (version 2.1.0) (Kim *et al.*, 2019) together with Samtools (version
292 1.9) (Li *et al.*, 2009) with default parameters. The mapping results were then submitted to featureCounts
293 (Liao *et al.*, 2014) to calculate the TPM (tags per million reads) values to estimate the level of gene
294 expression in each sample. To investigate the expression pattern of gene *Capana12g000954* in
295 accessions with different fruit orientations, we sampled the flower, fruit, leaf, root, and stem organs
296 from two accessions (erect vs pendent), which were then sequenced and analysed using the
297 aforementioned methods.

298

299 ***BSA-Seq and data analysis***

300 A wild pepper (*C. annuum* var. *glabriusculum*) accession Ac1979 with erect fruit was crossed with a
301 blocky pepper accession Qiemen with pendent fruit to construct an F₂ population of ~360 plants. 30

302 plants exhibiting the erect and 30 exhibiting the pendent fruit phenotypes were selected from the
303 population. DNA from the parents and the two F₂ groups was extracted, and the later were further
304 combined into two pools for library construction. The resulting libraries were sequenced on the MGI's
305 DNBSEQ-T7 platform from BGI-Shenzhen Company (Shenzhen, China). Clean reads were mapped
306 to the Zunla-1 2.0 genome and the variants were called following the same method described above.
307 Low quality (Q < 20, DP < 5) or multi-allelic variants were filtered out, and the homozygous SNPs that
308 showed polymorphism between the two parents were obtained using an in-house Perl script. The ΔSNP-
309 index was calculated based on a 500 kb sliding window with a 50 kb increment as described previously
310 (Zhang et al., 2020).

311

312 **Quantitative RT-PCR analysis of candidate genes of pepper fruit orientation**

313 For qRT-PCR analysis of the gene *Capana12g000954*, total RNA was extracted from erect and pendent
314 peppers from following tissues: leaves, flower buds, flowers and flower pedicels at 3 d post-pollination,
315 fruits and fruit pedicels at 7 d post-pollination. Samples were immediately frozen in liquid nitrogen for
316 at least 30 s and then stored at -80°C. The RNA isolation and cDNA synthesis were performed using an
317 SV Total RNA Isolation System kit (Promega) and the GoScript™ Reverse Transcription System kit
318 (Promega), respectively, according to the manufacturer's instructions. Gene expression analysis was
319 performed by qRT-PCR with the LightCycler®480 SYBR Green I Master on a LightCycler®480 II
320 (Roche) real-time PCR system. The *Capsicum actin* (*GQ339766.1*) and *EF1a* (*AY496125*) were used
321 as reference genes. The primers (F- AGTTATGCAAGCTCTGATCTGT and R-
322 TGTTGTTTCATAGACGGGCA) were designed online (<https://primer3.ut.ee/>). The qRT-PCR was
323 performed with two biological and three technical repetitions and each reaction was repeated three
324 times. The same method was used to analyze gene silencing in the VIGS experiment.

325

326 **Virus-induced gene silencing (VIGS)**

327 VIGS was used to verify the function of the *up* gene *Capana12g000954*. We selected the specific
328 sequence region (4 bp-303 bp) of 5' *Capana12g000954* to construct the VIGS vector. We confirmed
329 the sequence specificity by BLAST searching of the Zunla genome databases. A 300 bp fragment of
330 *Capana12g000954* was cloned from a pepper cDNA template using gene specific primers F-
331 TGAGTAAGGTTACCGAATTCCAAGCTGGCCAAGAGAAGAA and R-
332 GGAGGCCTTCTAGAGAATTCCCTCCAGGAGAAATCTGCTTA, containing an *EcoRI* site. The
333 resulting product was inserted into the *EcoRI* site of pTRV2, to construct TRV2::*up*. A fragment of
334 about 100 bp of *CaPDS* gene was inserted into pTRV2 to construct the control vector TRV2::*CaPDS*.
335 The tobacco rattle virus (TRV)-based vectors TRV1 and TRV2::*rec* were transformed into
336 *Agrobacterium tumefaciens* (strain GV3101) for infiltration. Bacteria were grown and resuspended in
337 infiltration solution at an OD₆₀₀ of about 4.0. After standing at room temperature for 3 hours, the
338 *Agrobacterium* suspensions containing the TRV1 vector and one of the TRV2 vectors (TRV1+TRV2;
339 TRV1+TRV2::*CaPDS*; TRV1+TRV2::*up*) were mixed at a ratio 1:1 and infiltrated. 2-month old plants
340 of the accession "Changyang chili" (pendent fruit) was used for VIGS experiments. The plant growth
341 environment was 23±2°C, the relative humidity was 60%-80%, and the light was 16h/8h (light/dark).
342 After infiltration, the plants were placed in the dark and cultured for 24h and then reverted to 16/8h
343 light-dark alternate culture. Five plants were used for each of the three groups (non-infiltrated,
344 TRV2::00, and TRV2::*up* experiments. Only plants infiltrated with TRV2::*up* plants showed fruits with
345 erect orientation, two months after infiltration. To investigate the expression of the *up* gene, total RNA
346 was isolated from pendent fruit pedicels of wild type and TRV2::00 and from erect pedicels of
347 TRV2::*up* plants. Gene expression analysis was performed by the qRT-PCR method described above.
348 Four biological replicates (pedicels) and four technical replicates were performed.

349

350 ***Bisulfite sequencing and DNA methylation analyses***

351 To determine the methylation levels of the 579 bp sequence in the promoter region of
352 *Capana12g000954*. Bisulfite treatment of genomic DNA from erect pepper was conducted using EpiArt
353 DNA Methylation Bisulfite Kit according to the manufacturer's instructions (Vazyme). Un-methylated
354 cytosine (C) was converted into uracil (U), which was further interpreted as thymine (T). Treated DNA
355 was used for PCR amplification using specific primers (F:
356 AGTTAAATAAAGAAAGGTTTAGTGAAAT, R: TTTTATCCCTATCTATTAACCATAAAAC).
357 PCR conditions were as follows: 98 °C for 30 s; 35 cycles of 98 °C for 10 s, 53 °C for 5 s, and 72 °C
358 for 15 s and 72 °C for 1 min. The PCR products were then sequenced to determine the methylation
359 status of C loci.

360

361

362 **Supplementary Tables**

363

364 **Table S1.** Summary of the sampled collection of pepper.

365 Presented in the spreadsheet file.

366

367 **Table S2.** SNP loci verification by Kompetitive Allele-Specific PCR (KASP).

368 Presented in the spreadsheet file.

369

370 **Table S3.** Positions of the SNPs and InDels identified in the pepper population*.

Variant	Genic						Intergenic	Total
	CDS		Intron		UTR			
	NS/FS	S/NFS	splice	intron	5'UTR	3'UTR		
SNP	55,711	33,346	471	274,840	464,143	386,470	17,157,041	18,372,022
INDEL	2,027	900	153	27,197	39,799	33,621	699,539	802,875

371 **: Abbreviations: CDS: coding sequences; UTR: untranslated region; NS: nonsynonymous and S:*
372 *synonymous mutations of SNPs; FS: frameshift and NFS: non-frameshift mutations of InDel.*

373

374

375 **Table S4.** Genomic regions under selection in transitions between different *C. annuum* groups,
 376 measured by ROD (reduction of diversity).

Groups (a vs. b)*	Chromosome	Start	Stop
II vs. I	Chr02	1	3,500,001
II vs. I	Chr04	80,500,002	100,500,001
II vs. I	Chr08	55,500,002	91,500,001
II vs. I	Chr09	127,500,002	185,500,001
II vs. I	Chr11	86,500,002	102,500,001
II vs. I	Chr11	105,500,002	106,500,001
III vs. II	Chr04	144,500,002	152,500,001
III vs. II	Chr05	166,500,002	169,500,001
III vs. II	Chr05	171,500,002	181,500,001
III vs. II	Chr05	188,500,002	205,500,001
III vs. II	Chr07	82,500,002	91,500,001
III vs. II	Chr07	129,500,002	180,500,001
III vs. II	Chr10	85,500,002	106,500,001
III vs. II	Chr12	88,500,002	104,500,001
III vs. II	Chr12	144,500,002	145,500,001
VII-IX vs. II	Chr04	127,500,002	138,500,001
VII-IX vs. II	Chr06	154,500,002	155,500,001
VII-IX vs. II	Chr06	159,500,002	164,500,001
VII-IX vs. II	Chr06	169,500,002	170,500,001
VII-IX vs. II	Chr07	82,500,002	90,500,001
VII-IX vs. II	Chr09	64,500,002	72,500,001
VII-IX vs. II	Chr09	124,500,002	128,500,001
VII-IX vs. II	Chr09	131,500,002	144,500,001
VII-IX vs. II	Chr11	143,500,002	150,500,001
VII-IX vs. II	Chr12	75,500,002	151,500,001
IV,VI vs. III	Chr07	130,500,002	158,500,001
IV,VI vs. III	Chr08	62,500,002	77,500,001
IV,VI vs. III	Chr08	93,500,002	96,500,001
IV,VI vs. III	Chr10	74,500,002	106,500,001
IV,VI vs. III	Chr11	61,500,002	105,500,001
IV,VI vs. III	Chr11	124,500,002	137,500,001

377 * *Group a compared to its progenitor group b.*

378

379

380 **Table S5.** Significantly enriched GO (gene ontology) terms in genes under selection transitions between
 381 different *C. annuum* groups. Note: GO functions colored in red indicate important candidate gene sets
 382 involved in pepper fruit evolution.

383 Presented in the spreadsheet file.

384

385 **Table S6.** Gene units under selection in different pepper groups compared to their progenitor groups in
 386 the pepper population.

Gene	ROD	π_a	π_b	#SNPs	Gene symbol/annotation	Groups (a vs. b)*
<i>Capana04g002188</i>	0.92	0.03	0.44	62	AP2-A, sepal regulation	II vs. I
<i>Capana02g000700</i>	0.98	0.01	0.48	78	AP2-A, sepal regulation	III vs. II
<i>Capana05g000060</i>	1	0	0.3	15	SUN, SHQD12, fruit shape regulation	IV, VI vs. III
<i>Capana07g001005</i>	1	0	0.47	33	agamous family gene, flower development related	IV, VI vs. III
<i>Capana10g000984</i>	0.96	0.02	0.43	73	cyclin-dependent protein kinase	IV, VI vs. III
<i>Capana10g001014</i>	0.96	0.02	0.44	35	cyclin-dependent protein kinase	IV, VI vs. III
<i>Capana03g002426</i>	0.72	0.1	0.35	52	mitotic phase inducer phosphatase-like protein	IV, VI vs. III
<i>Capana09g001401</i>	0.79	0.06	0.31	191	glycine-rich cell wall structural protein-like	IV, VI vs. III

387 * *Group a compared to its progenitor group b.*

388

389

390 **Table S7.** The expression of up gene (Capana12g000954) in different organs of pepper samples with
391 erect or pendent fruits.

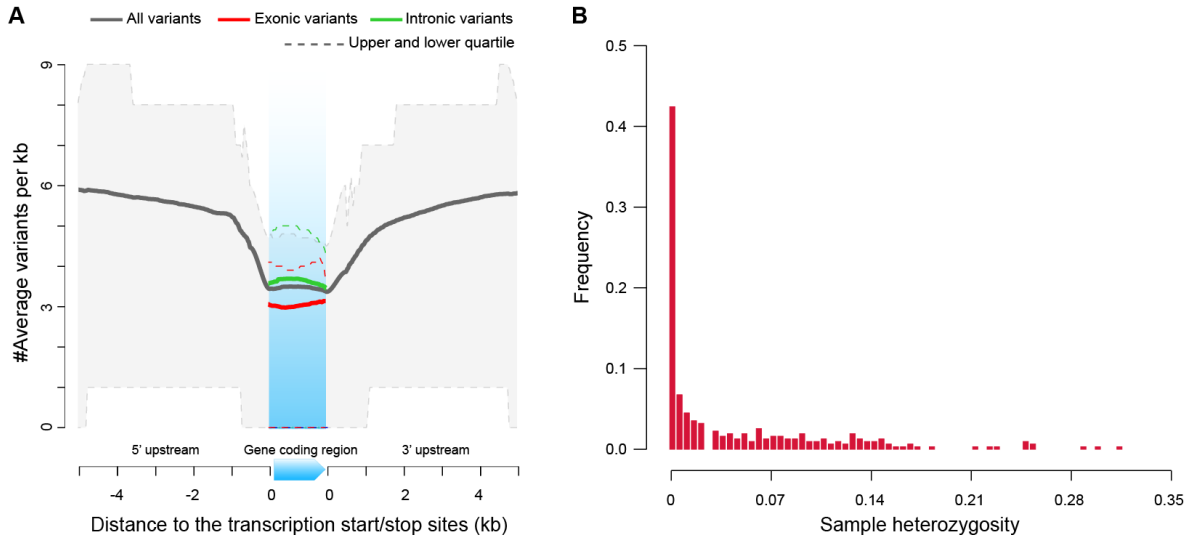
Type	Leaf*	Stem	Root	Flower	Fruit
Erect	0.08	0.76	0.36	50.19	2.18
Pendent	0.00	2.00	2.43	23.99	35.83

392 *: The gene expression values were estimated by TPM (Transcripts Per kilobase of exon model per
393 Million mapped reads).

394

395 **Supplementary Figures**

396



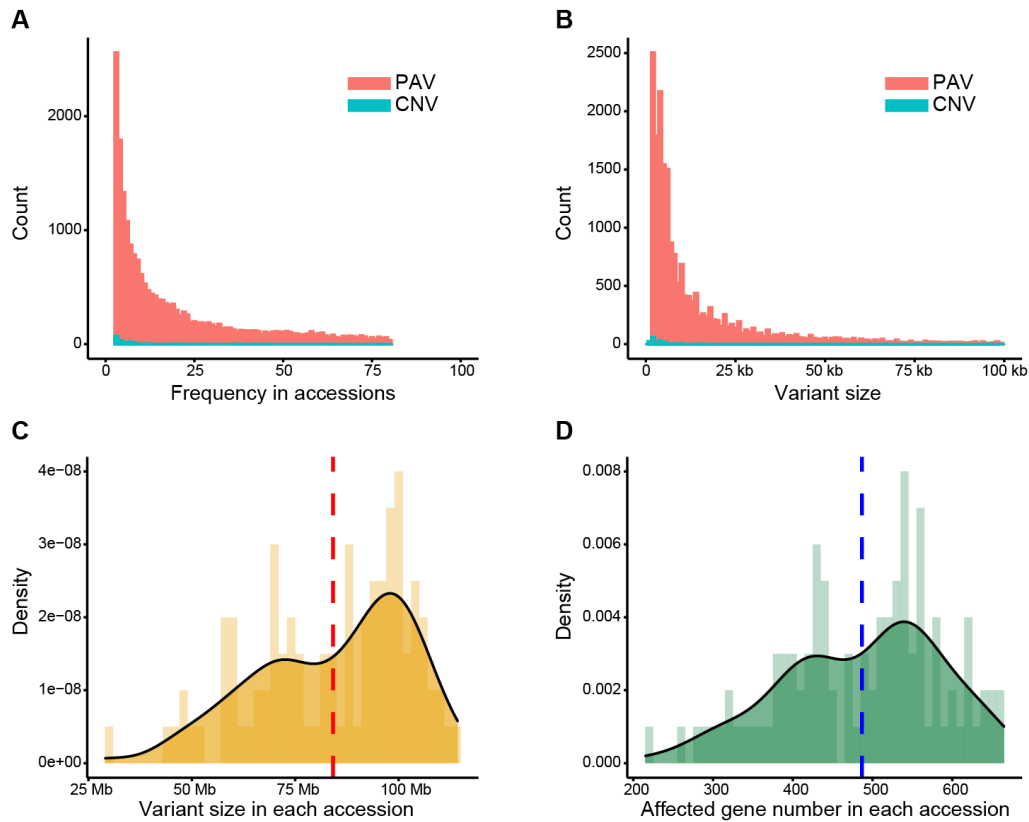
397

398

399 **Fig. S1.** (A) Density of the variants in the gene bodies and the 5 kb gene-flanking regions in the *C.*
400 *annuum* population. (B) Frequency distribution of the sample heterozygosity in the resequenced pepper
401 population.

402

403



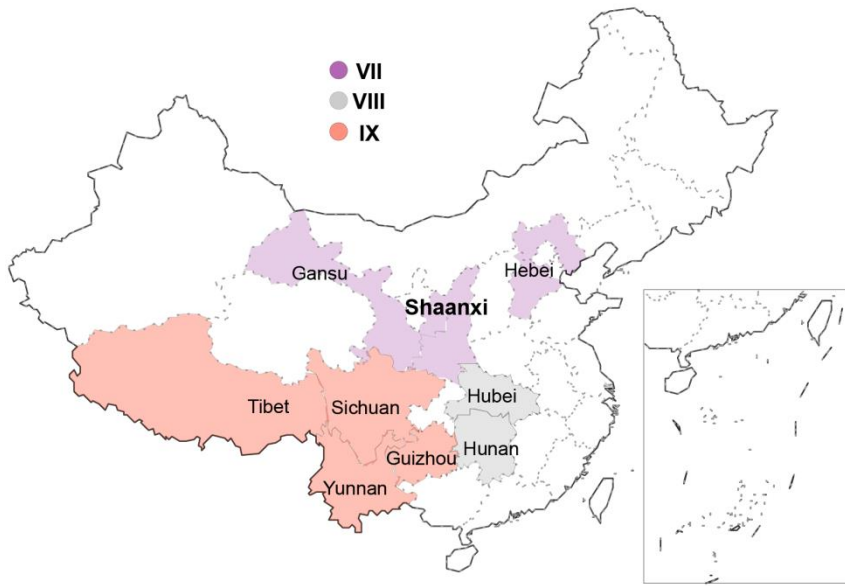
404

405

406 **Fig. S2.** Characteristics of the identified PAVs and CNVs in 100 pepper accessions. The numbers of
 407 PAVs and CNVs with different frequency in 100 accessions (**A**) and with different size (**B**). Density
 408 distributions of PAV/CNV size (**C**) and affected gene number (**D**) in each accession. The average size
 409 and the affected gene number are indicated by the dashed lines.

410

411



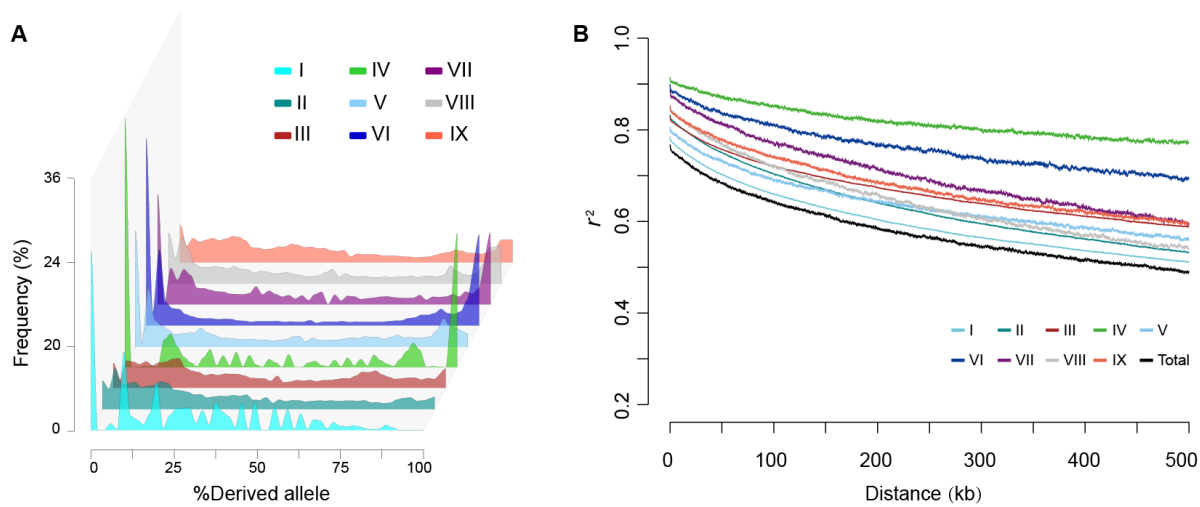
412

413

414 **Fig. S3.** Locations of China inland pepper groups VII, VIII, and IX in provinces from the north, middle
 415 and southwest of China.

416

417



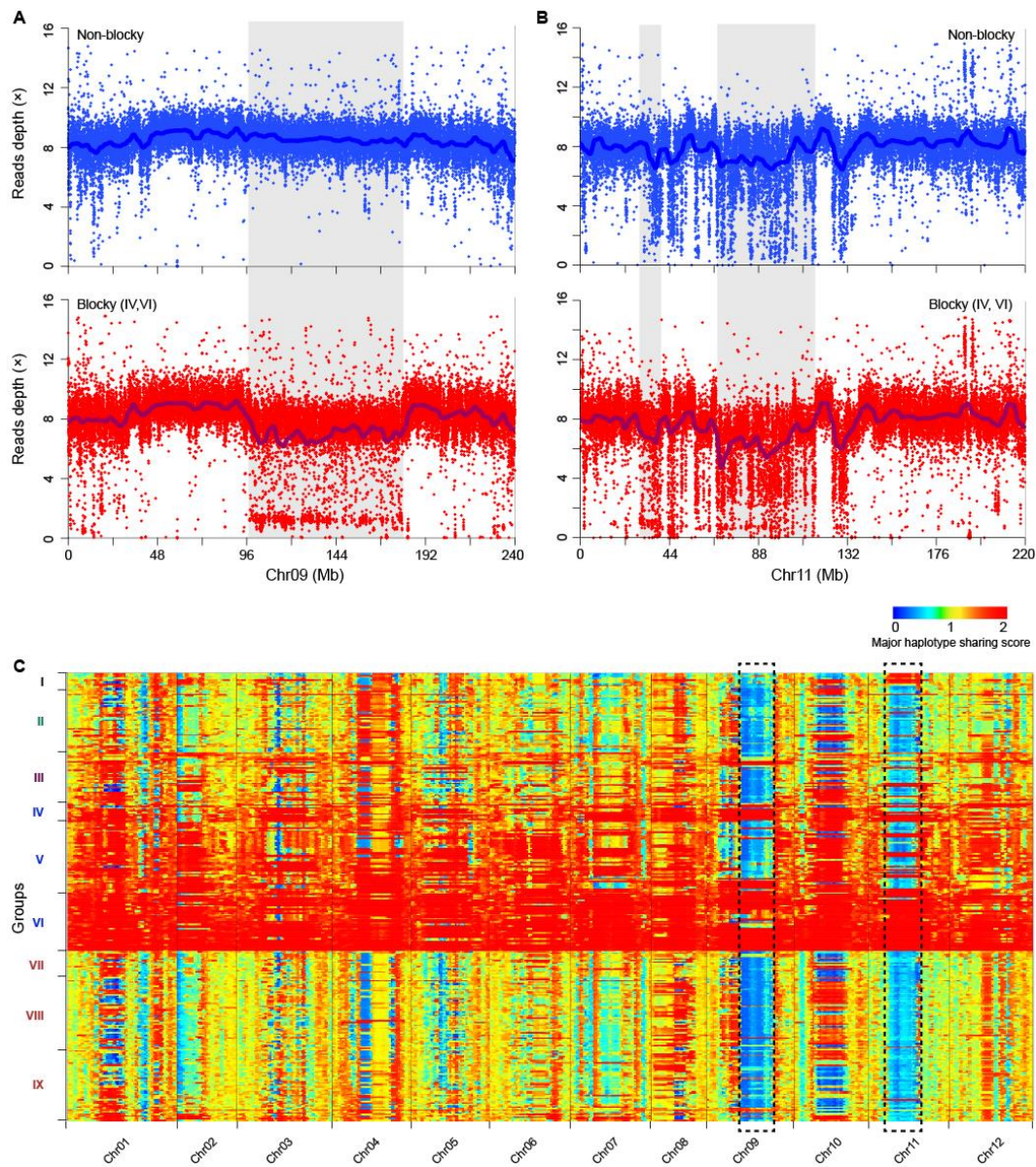
418

419

420 **Fig. S4.** (A) Frequency distribution of derived alleles of all SNPs in the nine pepper groups. (B) Decay
 421 of genomic linkage disequilibrium (LD) in the total *C. annuum* population, and in the nine groups (I-
 422 IX).

423

424



425

426

427 **Fig. S5.** The difference on depth of reads mapped to chromosomes 9 (A) and 11 (B) between the blocky
 428 and non-blocky fruit peppers. Blue and red points indicate average reads depth in 10 kb windows, dark
 429 blue lines denote average reads depth in 1 Mb window, and grey rectangles indicate the genomic regions
 430 showing lower depth of reads mapped to blocky fruit peppers. (C) Genome-wide haplotype sharing
 431 between blocky and non-blocky fruit peppers, with the major haplotype of the blocky fruit pepper as
 432 the reference. The y-axis lists samples following the same order as shown in main-text **Fig. 1C-D**. The
 433 heatmap colored from blue to red denotes low to high levels of major haplotype sharing score (MHS)
 434 of each sample to the major haplotype of blocky fruit pepper in a 10 Mb window across the whole
 435 genome.

436

437



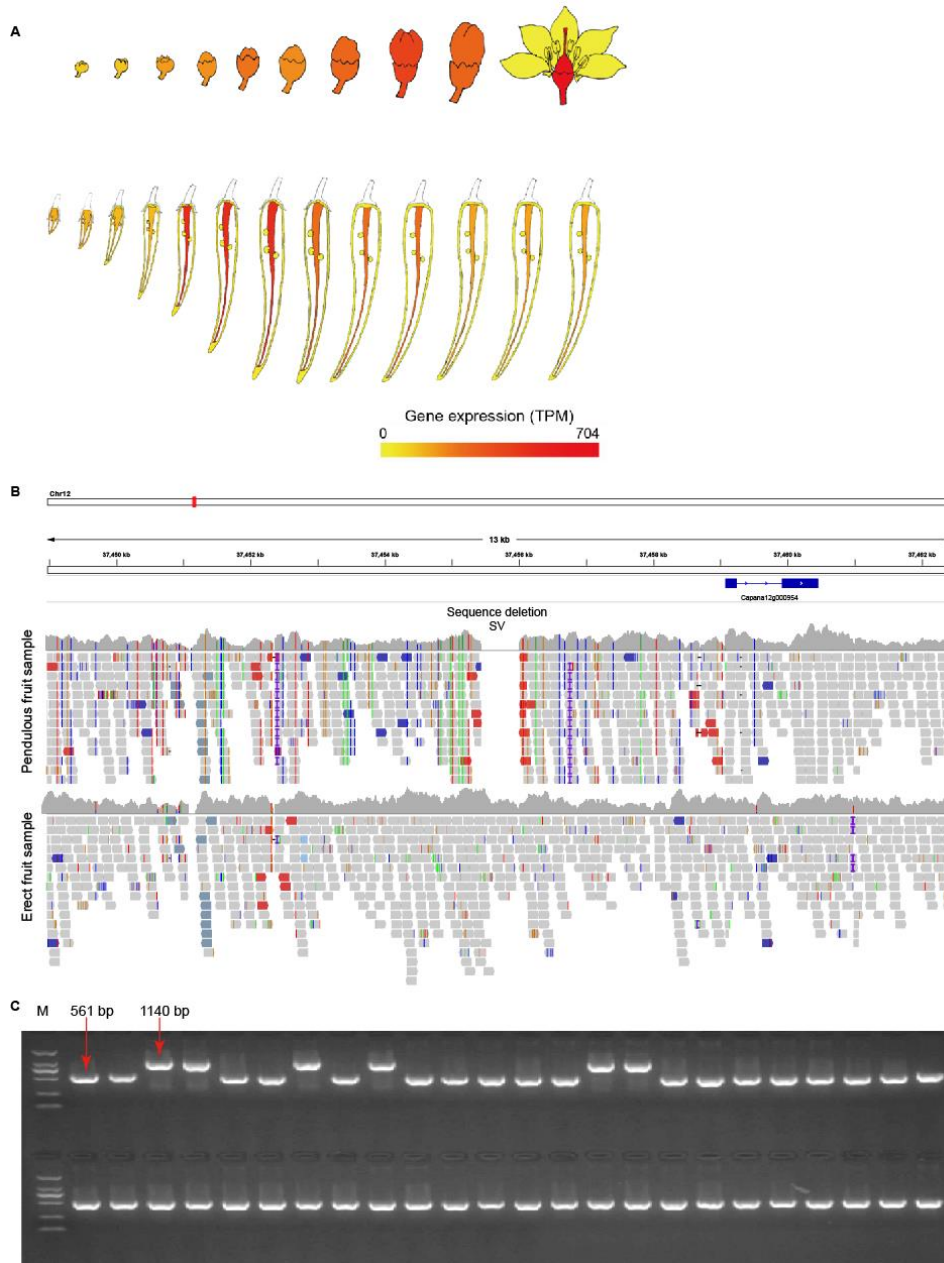
438

439

440 **Fig. S6.** Phylogenetic tree of the *C. annuum* population plus *C. annuum* var. *glabriusculum* whose
 441 genome has been released previously (Qin *et al.*, 2014), using genotypes of loci located at F9.

442

443

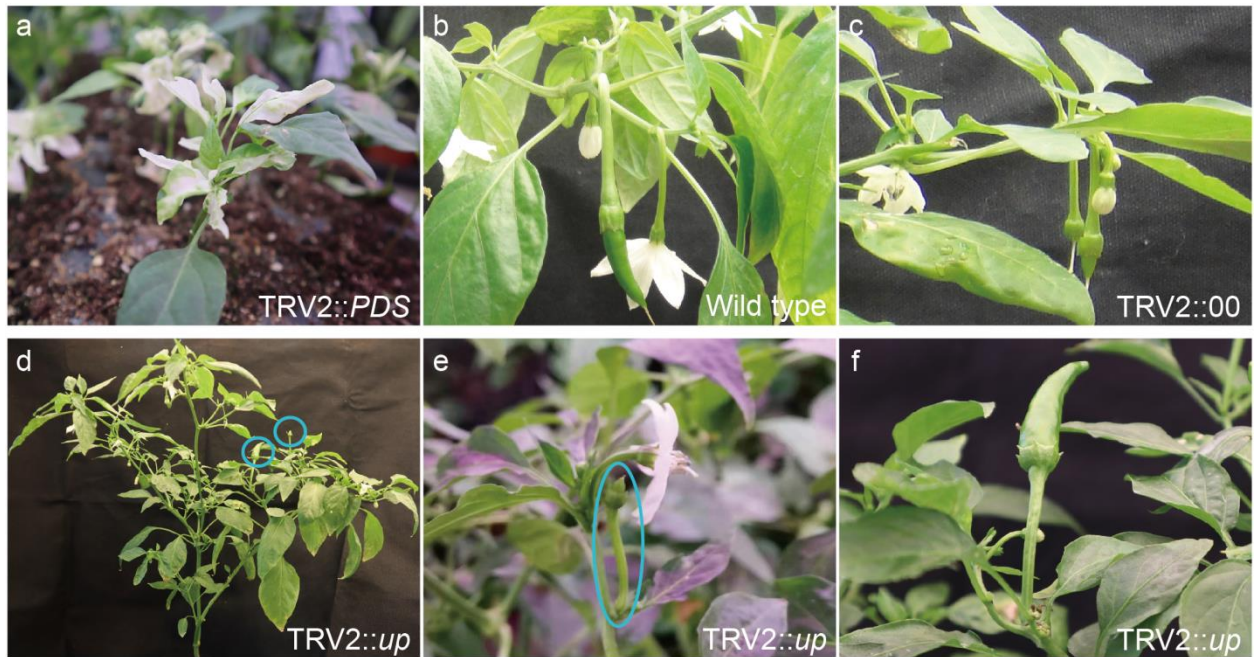


444

445 **Fig. S7.** (A) Gene expression of *Capana12g000954* (*Up*) in different developmental stages of pepper
 446 flower and fruit (Liu et al., 2017). (B) Visualization example of reads mapped onto the genomic region
 447 around gene *Capana12g000954* (*Up*) between samples with pendent (top) and erect (bottom) pepper
 448 fruits. The region that was not covered by any reads in the pendent fruit pepper indicates a large
 449 sequence deletion corresponding to the 579 bp deletion. (C) Electropherogram of the PCR products that
 450 cover the deletion upstream of gene *Capana12g000954* (*Up*) in different pepper samples. The 561 bp
 451 electrophoretic bands indicate samples with the 579 bp sequence deletion, while the 1,140 bp bands
 452 indicate samples without the sequence deletion. M: DNA marker DM2000.

453

454



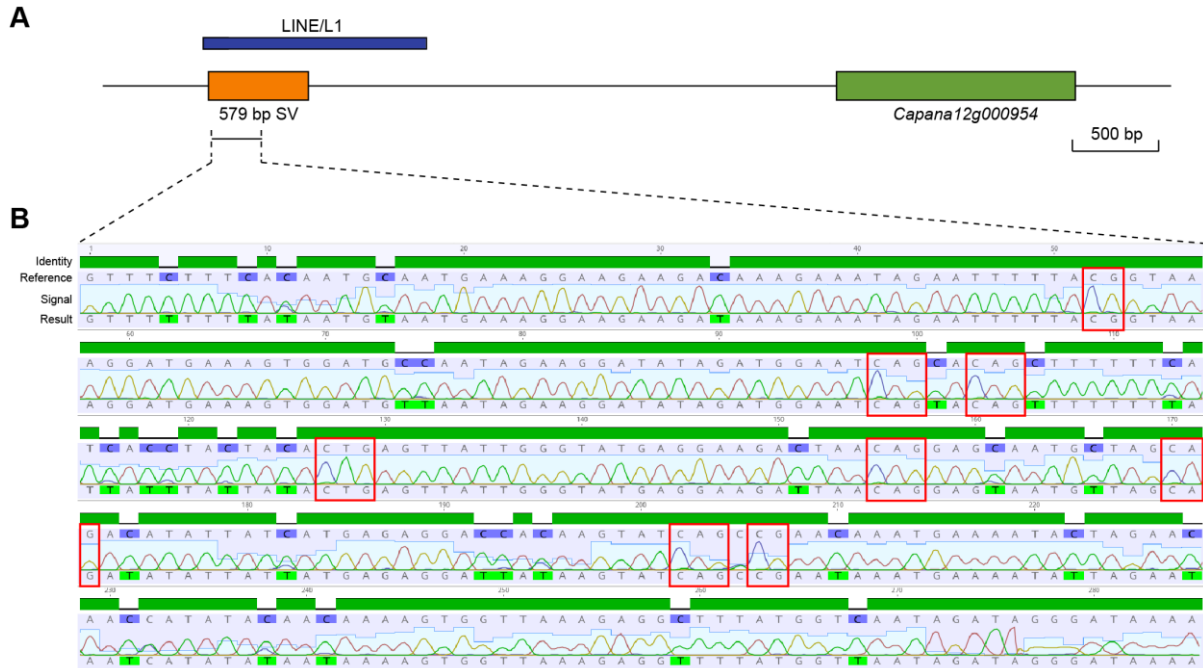
455

456

457 **Fig. S8.** The phenotypes of virus-induced gene silencing experiments on pepper accession “Changyang
 458 chili” with pendent fruit (wild type). (a) The TRV2::CaPDS pepper plant shows photobleaching; (b)
 459 Pendent fruit observed in the control plant (wild type); (c) Pendent fruit observed in plants treated with
 460 empty vector (TRV2::00); (d) Whole plant treated with TRV2::up, exhibiting with erect fruits; (e)
 461 Close-up of an erect flower and a small erect pepper fruit in a plant treated with TRV2::up; (f) Close-
 462 up of a large erect pepper fruit in a plant treated with TRV2::up.

463

464



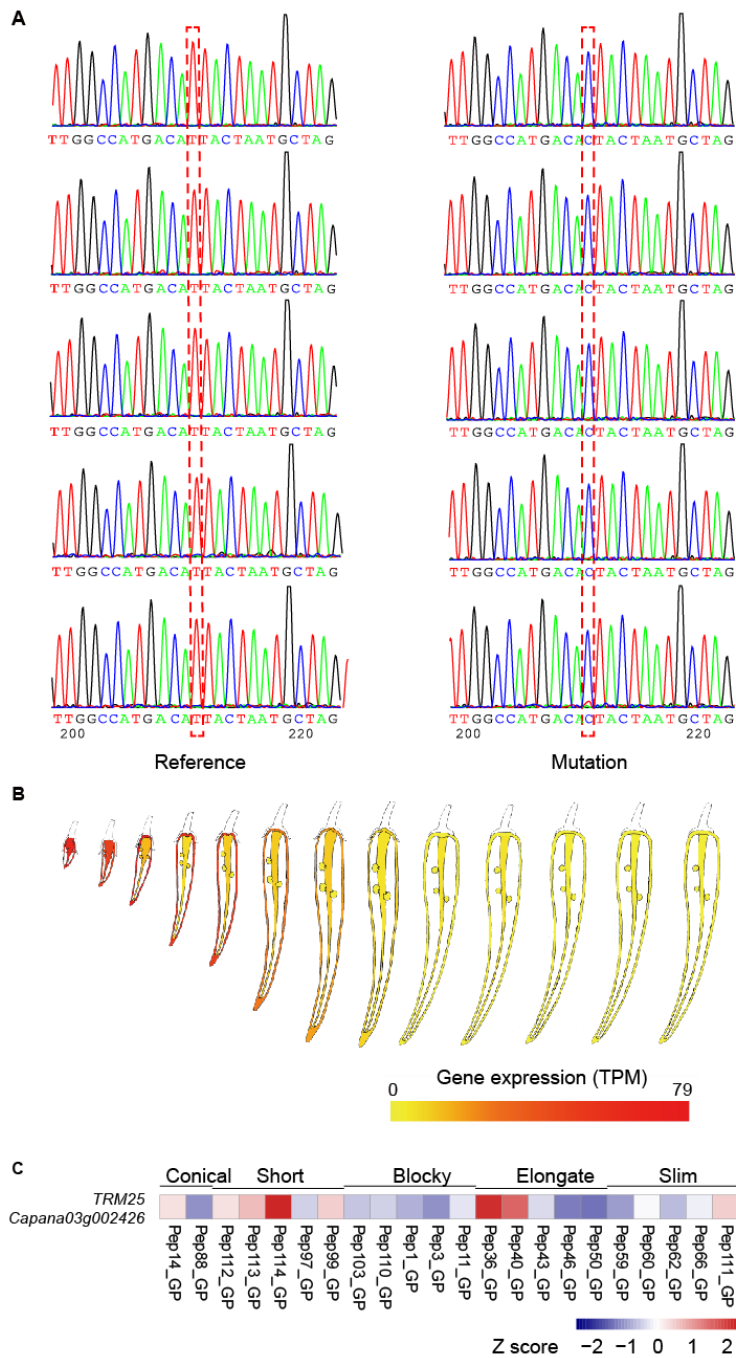
465

466

467 **Fig. S9.** DNA methylation status of the 579 bp SV in the promoter region of *Capana12g000954*. (A)
 468 Diagram illustrating the relative positions of the SV (orange), the overlapped TE (navy blue), and the
 469 *Capana12g000954* (green). The region bordered by dashed line was selected to do bisulfite sequencing
 470 to estimate the methylation status of the deleted sequence. (B) Comparison of the reference sequence
 471 and the bisulfite treated sequence with the un-methylated cytosine (C) converted into thymine (T). The
 472 Cs, especially those locating at the CpG and CHG sites (red box), in this region were heavily
 473 methylated, since they kept unchanged as Cs (purple signal) after bisulfite treatment.

474

475

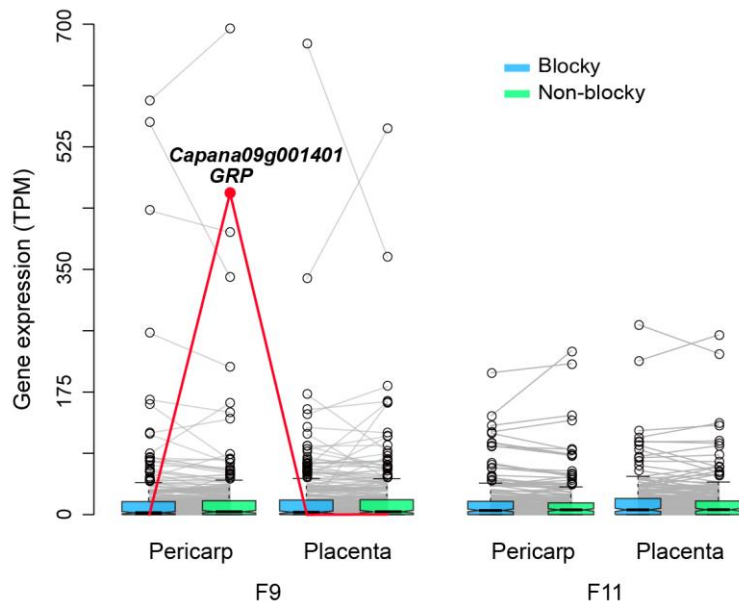


476

477 **Fig. S10.** (A) Sanger sequencing of the nonsynonymous mutation in *TRM25* in the test population. The
 478 red dashed-line rectangle denotes the position of the mutation. (B) Gene expression of
 479 *Capana03g002426* (*TRM25*) in different developmental stages of pepper fruit (Liu *et al.*, 2017). (C)
 480 Expression heatmap of *Capana03g002426* (*TRM25*) in the pericarp of 22 accessions with different fruit
 481 types evaluated through RNA-Seq.

482

483



484

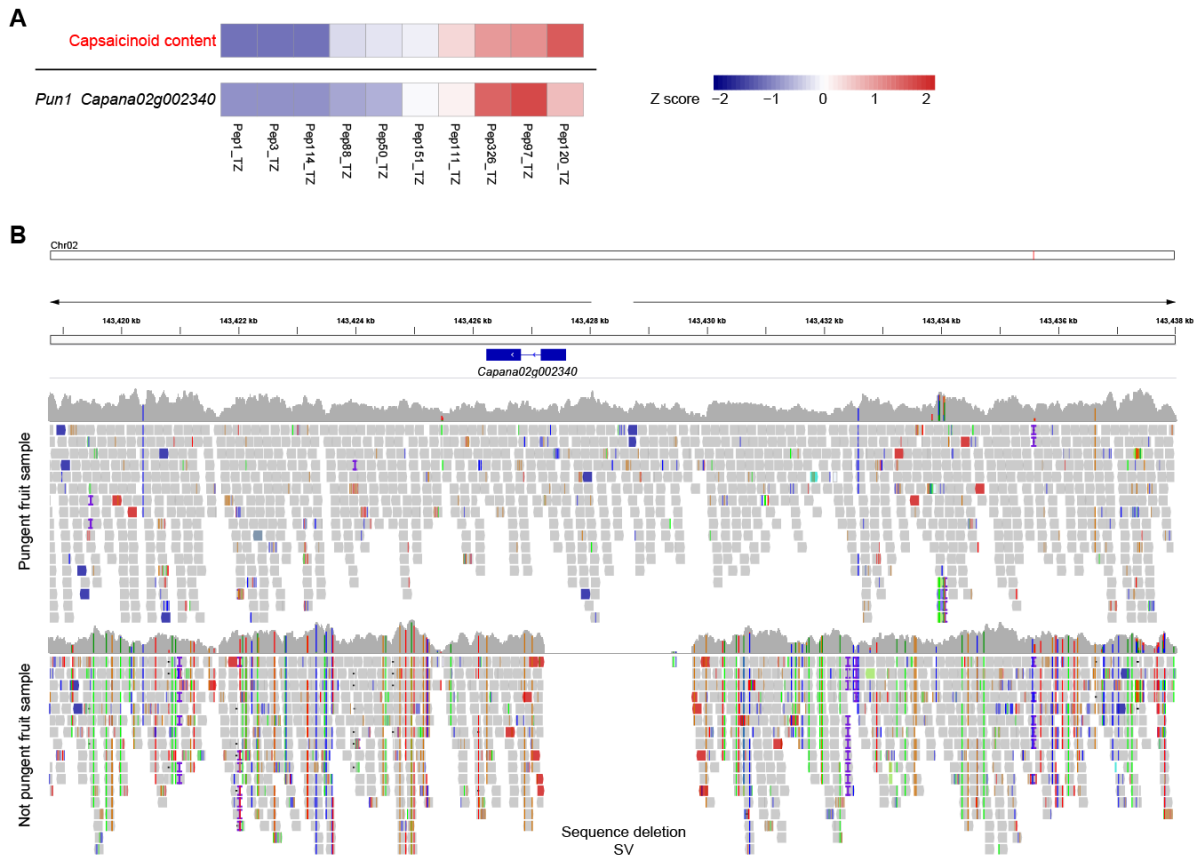
485

486 **Fig. S11.** Boxplot of gene expression for genes located at F9 and F11 in two pepper fruit tissues
 487 (pericarp and placenta) between blocky and non-blocky fruit peppers. The lines link the same genes in
 488 different boxplots; the red line indicates the gene *Capana09g001401* that is highly and specifically
 489 expressed in the pericarp of non-blocky fruit pepper. TPM: tags per million reads.

490

491

492



493

494

495

496

497

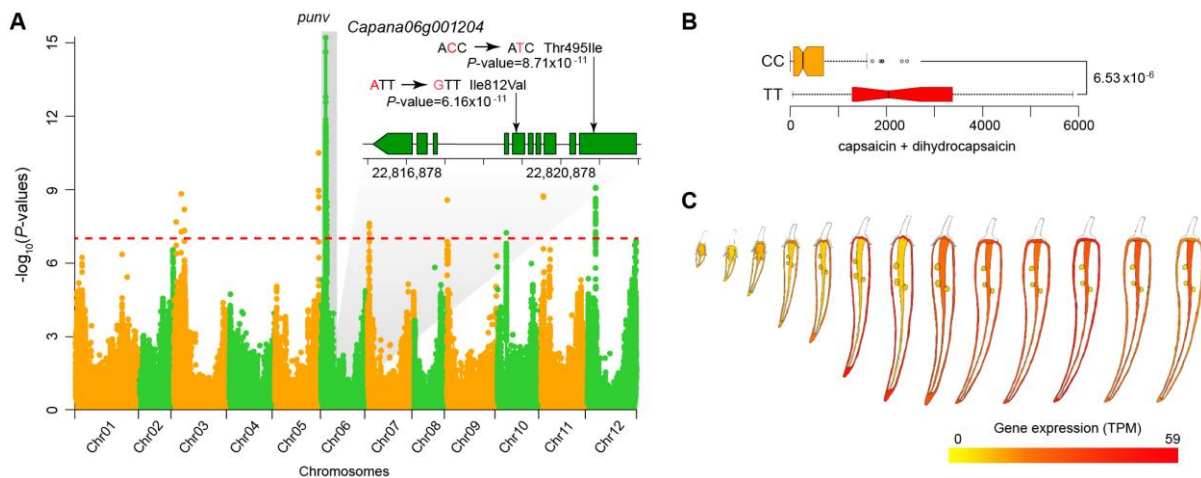
498

499

500

501

Fig. S12. (A) Expression heatmap of *Capana02g002340* (*Pun1*) in the placenta of 10 accessions with different capsaicinoid content evaluated through RNA-Seq. (B) Mapping of reads mapped onto the genomic region around gene *Capana02g002340* (*Pun1*) between peppers with pungent (top) and non-pungent (bottom) fruits. The region that was not covered by any reads in non-pungent fruit peppers, indicating a large sequence deletion.



502

503

504 **Fig. S13.** The mapping of genomic loci associated with the pungency variation in the narrow-fruit
 505 pepper. (A) GWAS identified a locus *punv* that showed association signal of capsaicinoid content, and
 506 there were two (Thr495Ile and Ile812Val) mutations in the candidate gene *Capana06g001204*; (B)
 507 differences in capsaicinoid content in genotypes carrying the nonsynonymous mutations, in GWAS and
 508 test populations. (C) *Capana06g001204* expression during development of the pepper fruit.

509

510

511

512 SI References

513

514 **Akey, J.M., Zhang, G., Zhang, K., Jin, L., and Shriver, M.D.** (2002). Interrogating a high-
 515 density SNP map for signatures of natural selection. *Genome Research* **12**:1805-1814.
 516 [10.1101/gr.631202](https://doi.org/10.1101/gr.631202).

517 **Browning, B.L., Zhou, Y., and Browning, S.R.** (2018). A One-Penny Imputed Genome
 518 from Next-Generation Reference Panels. *The American Journal of Human Genetics* **103**:338-
 519 348. [10.1016/j.ajhg.2018.07.015](https://doi.org/10.1016/j.ajhg.2018.07.015).

520 **Edgar, R.C.** (2004). MUSCLE: a multiple sequence alignment method with reduced time
 521 and space complexity. *BMC Bioinformatics* **5**:113. [10.1186/1471-2105-5-113](https://doi.org/10.1186/1471-2105-5-113).

522 **Gu, X.-z., Cao, Y.-c., Zhang, Z.-h., Zhang, B.-x., Zhao, H., Zhang, X.-m., Wang, H.-p.,
 523 Li, X.-x., and Wang, L.-h.** (2019). Genetic diversity and population structure analysis of
 524 *Capsicum* germplasm accessions. *Journal of Integrative Agriculture* **18**:1312-1320.
 525 [https://doi.org/10.1016/S2095-3119\(18\)62132-X](https://doi.org/10.1016/S2095-3119(18)62132-X).

526 **Guy St C, S., and Ewan, B.** (2005). Automated generation of heuristics for biological
 527 sequence comparison. *BMC Bioinformatics* **6**:31-31. [10.1186/1471-2105-6-31](https://doi.org/10.1186/1471-2105-6-31).

528 **Haas, B.J., Salzberg, S.L., Zhu, W., Pertea, M., Allen, J.E., Orvis, J., White, O., Buell,
 529 C.R., and Wortman, J.R.** (2008). Automated eukaryotic gene structure annotation using
 530 EVIDENCEModeler and the Program to Assemble Spliced Alignments. *Genome Biology* **9**:R7.
 531 [10.1186/gb-2008-9-1-r7](https://doi.org/10.1186/gb-2008-9-1-r7).

532 **Hoff, K.J., and Stanke, M.** (2018). Predicting Genes in Single Genomes with AUGUSTUS.
533 Current Protocols in Bioinformatics:e57. 10/gfpr44.

534 **Kim, D., Paggi, J.M., Park, C., Bennett, C., and Salzberg, S.L.** (2019). Graph-based
535 genome alignment and genotyping with HISAT2 and HISAT-genotype. Nat Biotechnol
536 **37**:907-915. 10.1038/s41587-019-0201-4.

537 **Krzywinski, M., Schein, J., Birol, I., Connors, J., Gascoyne, R., Horsman, D., Jones,
538 S.J., and Marra, M.A.** (2009). Circos: an information aesthetic for comparative genomics.
539 Genome Research **19**:1639-1645. 10.1101/gr.092759.109.

540 **Li, H., and Durbin, R.** (2009). Fast and accurate short read alignment with Burrows–
541 Wheeler transform. Bioinformatics **25**:1754-1760.

542 **Li, H., Handsaker, B., Wysoker, A., Fennell, T., Ruan, J., Homer, N., Marth, G.,
543 Abecasis, G., Durbin, R., and Genome Project Data Processing, S.** (2009). The Sequence
544 Alignment/Map format and SAMtools. Bioinformatics **25**:2078-2079.
545 10.1093/bioinformatics/btp352.

546 **Liao, Y., Smyth, G.K., and Shi, W.** (2014). featureCounts: an efficient general purpose
547 program for assigning sequence reads to genomic features. Bioinformatics **30**:923-930.
548 10.1093/bioinformatics/btt656.

549 **Liu, F., Yu, H., Deng, Y., Zheng, J., Liu, M., Ou, L., Yang, B., Dai, X., Ma, Y., Feng, S., et
550 al.** (2017). PepperHub, an Informatics Hub for the Chili Pepper Research Community.
551 Molecular Plant **10**:1129-1132. 10.1016/j.molp.2017.03.005.

552 **Lomsadze, A., Ter-Hovhannisyanyan, V., Chernoff, Y.O., and Borodovsky, M.** (2005). Gene
553 identification in novel eukaryotic genomes by self-training algorithm. Nucleic Acids Res
554 **33**:6494-6506. 10.1093/nar/gki937.

555 **Pritchard, J.K., Stephens, M., and Donnelly, P.** (2000). Inference of population structure
556 using multilocus genotype data. Genetics **155**:945-959.

557 **Qin, C., Yu, C., Shen, Y., Fang, X., Chen, L., Min, J., Cheng, J., Zhao, S., Xu, M., and
558 Luo, Y.** (2014). Whole-genome sequencing of cultivated and wild peppers provides insights
559 into *Capsicum* domestication and specialization. Proceedings of the National Academy of
560 Sciences of the United States of America **111**:5135-5140.

561 **Retief, J.D.** (2000). Phylogenetic analysis using PHYLIP. Methods in Molecular Biology
562 **132**:243-258.

563 **Sabeti, P.C., Varilly, P., Fry, B., Lohmueller, J., Hostetter, E., Cotsapas, C., Xie, X.,
564 Byrne, E.H., McCarroll, S.A., Gaudet, R., et al.** (2007). Genome-wide detection and
565 characterization of positive selection in human populations. Nature **449**:913-918.
566 10.1038/nature06250.

567 **Szpiech, Z.A., and Hernandez, R.D.** (2014). selscan: an efficient multithreaded program to
568 perform EHH-based scans for positive selection. Molecular Biology and Evolution **31**:2824-
569 2827. 10.1093/molbev/msu211.

570 **Tajima, F.** (1983). Evolutionary relationship of DNA sequences in finite populations.
571 Genetics **105**:437-460.

572 **Tajima, F.** (1989). Statistical method for testing the neutral mutation hypothesis by DNA
573 polymorphism. Genetics **123**:585-595.

574 **Wang, D., Zhang, Y., Zhang, Z., Zhu, J., and Yu, J.** (2010a). KaKs_Calculator 2.0: a
575 toolkit incorporating gamma-series methods and sliding window strategies. Genomics
576 Proteomics Bioinformatics **8**:77-80. 10.1016/S1672-0229(10)60008-3.

577 **Wang, H.P., Li, X.X., and Song, J.P.** (2018). Vegetable Genetic Resources in China.

578 Horticultural Plant Journal 4:83-88. 10.1016/j.hpj.2018.03.003.
579 **Wang, K., Li, M., and Hakonarson, H.** (2010b). ANNOVAR: functional annotation of
580 genetic variants from high-throughput sequencing data. Nucleic Acids Res 38:e164-e164.
581 **Xu, M., Guo, L., Gu, S., Wang, O., Zhang, R., Peters, B.A., Fan, G., Liu, X., Xu, X.,**
582 **Deng, L., et al.** (2020). TGS-GapCloser: A fast and accurate gap closer for large genomes
583 with low coverage of error-prone long reads. GigaScience 9:giaa094.
584 10.1093/gigascience/giaa094.
585 **Xu, X., Liu, X., Ge, S., Jensen, J.D., Hu, F., Li, X., Dong, Y., Gutenkunst, R.N., Fang, L.,**
586 **Huang, L., et al.** (2011). Resequencing 50 accessions of cultivated and wild rice yields
587 markers for identifying agronomically important genes. Nature Biotechnology 30:105-111.
588 10.1038/nbt.2050.
589 **Yang, Y., Zhang, K., Xiao, Y., Zhang, L., Huang, Y., Li, X., Chen, S., Peng, Y., Yang, S.,**
590 **Liu, Y., et al.** (2022). Genome Assembly and Population Resequencing Reveal the
591 Geographical Divergence of Shanmei (*Rubus corchorifolius*). Genomics, Proteomics &
592 Bioinformatics 10.1016/j.gpb.2022.05.003.
593 **You, F.M., Huo, N., Gu, Y.Q., Luo, M.C., Ma, Y., Hane, D., Lazo, G.R., Dvorak, J., and**
594 **Anderson, O.D.** (2008). BatchPrimer3: a high throughput web application for PCR and
595 sequencing primer design. BMC Bioinformatics 9:253. 10.1186/1471-2105-9-253.
596 **Zhang, X., Zhang, K., Wu, J., Guo, N., Liang, J., Wang, X., and Cheng, F.** (2020). QTL-
597 Seq and Sequence Assembly Rapidly Mapped the Gene *BrMYBL2.1* for the Purple Trait in
598 *Brassica rapa*. Scientific Reports 10:2328. 10.1038/s41598-020-58916-5.
599 **Zhou, X., and Stephens, M.** (2012). Genome-wide efficient mixed-model analysis for
600 association studies. Nature Genetics 44:821-824. 10.1038/ng.2310.
601
602
603
604
605